An Intelligent System for Analyzing Welding Defects using Image Retrieval Techniques

Raoul Pascal Pein[1], Joan Lu[1], John Birger Stav[2], Q. Xu[3], Miro Uran[4], Luboš Mráz[5]

[1]Department of Informatics,
University of Huddersfield
Huddersfield HD1 3DH, UK

[2]Faculty of Technology
Sør-Trøndelag University College
Trondheim, 7004, Norway

[3]Department of Mech. Engineering
University of Teesside
Middlesbrough, TS1 3BA, UK

[4]Welding Institute
Ljubljana, 1000, Slovenia

[5]Welding Research Institute
Bratislava, 83259, Slovakia

ABSTRACT

The development of new approaches in image processing and retrieval provides several opportunities in supporting in different domains. The group of welding engineers frequently needs to conduct visual inspections to assess the quality of welding products. It is investigated, if this process can be supported by different kinds of software. Techniques from a generic CBIR system have been successfully used to cluster welding photographs according to the severeness of visual faults. Similarity algorithms were used to automatically spot faults, such as cracks and gas pores.

INTRODUCTION

The techniques of Content-Based Image Retrieval (CBIR) systems can be applied in various disciplines. Not only image processing in computing areas such as image libraries [1, 2] can be beneficial, but also other application domains. For example, the importance of CBIR is especially increasing in medical applications, where a large amount of X-ray images are produced for diagnosis [3], as well as the engineering sectors, where investigations in 3D model retrieval has been addressed recently [4].

In the field of CBIR, the feature vector paradigm is a commonly used technique [5, 6]. Several different features have been developed to describe the most relevant content of images in a highly condensed way [7,8]. Instead of comparing the complete images, only this information is used. This allows for fast and considerably accurate image retrieval.

In welding industry, Non Destructive Testing (NDT) could produce a huge amount of images in the forms of photos, digital images or X-ray pictures containing different types of welding defects. These images are vital to assess the quality of industrial products. According to the definitions defined by ISO 6520, there are 80 defect types listed in the documents. For each type, the defects could be grouped or classified into different degrees of severity. However, advanced image retrieval techniques are rarely applied into the field of welding, particularly for analyzing welding defects taken by x-ray pictures. Traditionally, analyzing X-Ray pictures may involve expensive facilities, which is costing and time consuming [9]. Some welding defects in radiographics can be spotted by trained humans, but for all detail information, it is extremely difficult to be analyzed accurately, which provide a very good opportunity for computer based analysis. The key to success is to find a feature that describes a defect detailed enough to allow automated detection [10]. It follows that research into developing an advanced system for retrieving, analyzing, classifying and recognizing welding defects is of interest in both academic study and industrial applications.

A recent overview concerning the analysis of radiographic weld seam images has been published by da Silva and Domingo, split into image processing [11] and pattern recognition [12] tasks. The mentioned approaches cover several problems from general noise reduction to spotting and measuring the strength of specific welding defects. The research of Felisberto et al. [10] is concerned with the task of detecting defined objects within radiographic images, which is highly valuable information for further analysis. Otherwise, sophisticated and time-consuming fault detection algorithms are prone to extract information from the wrong areas, making it difficult to determine the optimal processing parameters.

The objective of this research is to develop an analysis tool to spot and measure welding defects with minimal effort to the user. The challenge of this research is to find alternative ways to spot defects without being affected by background noise. It is crucial to define classifiers that are able to distinguish between different image areas, such as background, metal sheets, pipes and welding seams. These classifiers can be used to find the regions-of-interest where detailed analysis can be applied. Further, the characteristics of each region are useful to find the best parameters.

METHODS EMPLOYED

In this investigation, methods from the CBIR field are employed to analyze radiographic images of various welding defects. ISO 6520 (Classification of geometric imperfections in metallic materials) is used as supporting document to distinguish different types of welding defects.

- Segmentation: i.e. an image is segmented into regions;
- Extraction: i.e. extract different kinds of feature vectors for each one.

These feature vectors describe the region with highly condensed information. For example, feature vectors may contain the histogram values of a region to describe the color distribution [7]. Wavelet coefficients are used to describe frequencies [8], shape information [13] etc. Extracted features can be compared to each other and be used in retrieval. The detailed description of using feature vector algorithms for fault detection is as follows.

The idea is to split the original image into several smaller sections. Each section represents one or more object classes. In the following, the original image is split into 10x10 regions and various feature extraction algorithms are run on each of them. The resulting data set allows for a comparison of each two sections according to particular feature vector characteristics. Dependent on the kind of feature vector used, an average feature may be computable, e.g. calculating the arithmetic or geometric mean of a vector.

An alternative approach based on pure pattern recognition is described in [14]. It performs several steps of image pre-processing on the input image to end up with a gray-scale image, where the relevant areas have considerably different values than the average value. The transformations include techniques such as median, edge detection and Hough transform. That approach is capable of measuring the exact diameter of gas pores and the length and width of cracks. Hence, the success of that solution is dependent on the fine-tuning of various parameters used to remove background noise. Also, overlapping defects cannot always be detected correctly, as it is difficult to detect the boundaries of each single one.

SYSTEM DESIGN

The system design considers several actions and user requirements as follows:

1. Load sample image
2. Segment image
3. Extract feature vectors from segments
4. Select query: either existing segment or specific feature vector
5. Compare each segment to the query and collect similarities
6. Analyze similarity pattern

Most processing is done automatically and the tuning parameters are supposed to be hidden to the user. The automated tasks include: image segmentation, image analysis, comparison of segments, highlighting possible defects. The user interaction is covered by: loading an image, optionally selecting an initial region-of-interest and manually checking the potential defect locations.

The proposed system provides a straightforward user interface. It can load images, which are then segmented and analyzed automatically. The user’s main task is to select a region of interest. Based on the underlying feature information, the system automatically compares this region to the others. The result is an image, where the similarity to the selected region is displayed. It is assumed, that a suitable feature vector is able to highlight regions with significantly different content, i.e. local defects or other objects.

A completely user-independent way to generate results is the automatic selection of a source region or the use of average feature values. The latter approach is expected to be most powerful in sample images with relatively large homogeneous areas and only a few different spots.

IMPLEMENTATION

The prototype has been developed completely in Java. It uses a couple of external libraries. The basic image processing is done with the help of the Java Imaging Utilities [15]. All CBIR related functionality is directly taken from the image retrieval system developed prior to this research [16].

Internally, the source image is chopped into rectangular segments of a pre-defined size (i.e. 10x10 pixels). For each segment, a feature extraction algorithm is applied and the vector is attached to the corresponding sub image. The generated ad-hoc image repository is stored in the main memory. All further analysis is then handled like a complete CBIR retrieval. The query contains the desired feature vector and all segments are compared to it, resulting in a similarity between 0.0 and 1.0. For each segment, a color is calculated based on the respective similarity. This color is then used in the visualization to show the difference of each segment to the original query.

The feature used consists of 12 stochastic moments of the image histograms [7]. As these values can be interpreted as the scalar parts of a feature vector, it is possible to calculate the mean value of multiple features, resulting in a single average vector. In this case, the simple arithmetic means of each component are calculated and used as a new query.

TESTING

Testing data prepared using two representative cases, i.e. (name), in welding defects. Testing is carried out in the following stages:

1. Collection of 25 digital radiographic sample images
2. Manual acquisition of defects
3. Software supported detection of cracks and gas pores
4. Software supported comparison analysis
5. Assessment of automatic query generation
6. Comparison of results

The reference system is the previously developed detection tool for gas pores and cracks [14]. Provided that the algorithm parameters are set accordingly, the detection works with a reasonable precision. Regions detected in that tool should also be spotted in the proposed tool, which is using histogram-based CBIR algorithms. The samples contain different kinds of defects and are analyzed as described above.

Tthe regions spotted manually and by the two tools are compared according to their calculated significance. Further, the results of the automatic query generation are compared to the previous detection methods.

The testing has been carried out on a Intel CoreDuo PC with 2 GHz and 2 GB of main memory. The operating system is Windows XP and the Java environment is the current version 1.6.

RESULTS

Two representative test cases are presented below. For the first one, a sample image with a T-shaped welding seam, showing a crack, is used. It is to measure the ability of spotting a single defect in an inhomogeneous envoironment. For the second test case, a welding with several cracks and gas pores is chosen. The smooth background is expected to be suitable to calculate a suitable mean value, representing the intact area.

CASE ONE: SINGLE CRACK

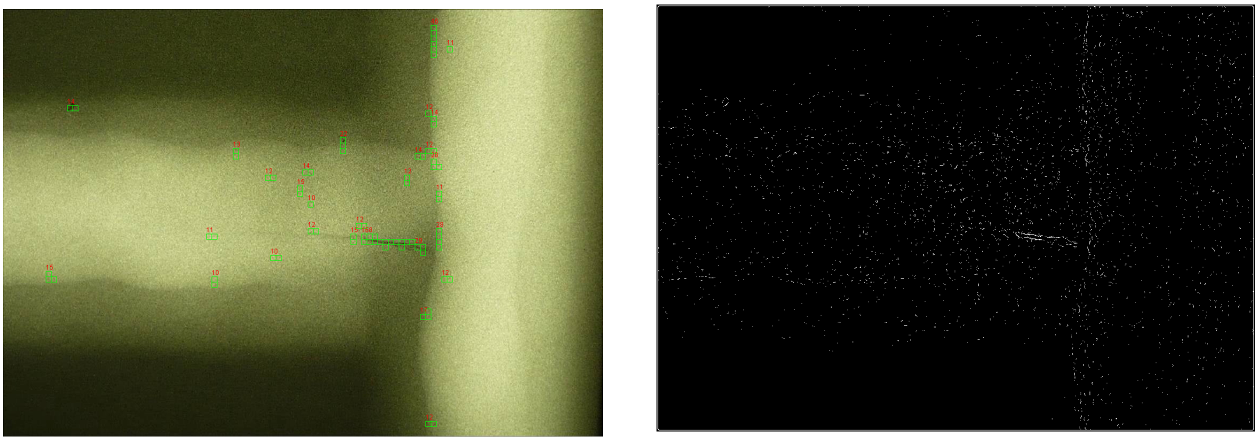

(a) spotted regions-of-interest (b) edge detection result

Figure 1: pattern recognition on T-shaped seam

In Figure 1, a T shaped welding seam is depicted. There is an obvious crack in the central part running orthogonally from the centre to the second seam. This crack clearly emerges from the corresponding black/white image and can be spotted against the noise. The vertical seam on the right appears as a dotted line.

After procesing, the crack itself is enclosed within 4 clusters, while the largest cluster contained in the image (ranking of 168) is located directly on the main part of the crack. The second largest cluster (ranking of 46) is a straight part of the vertical seam. Several small clusters (ranking below 30) are scattered across the whole image.

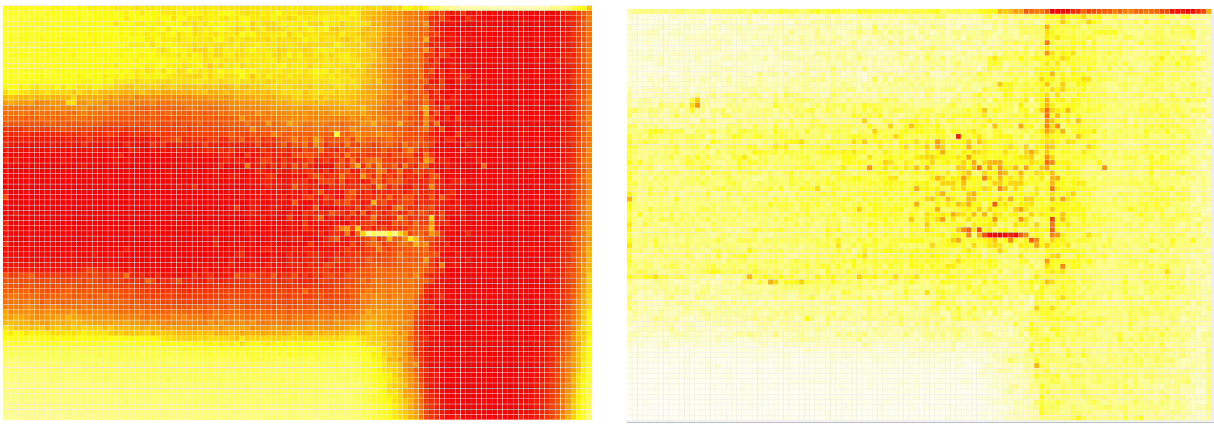

(a) highlighted seam (b) highlighted crack

Figure 2: similarity results on T-shaped seam

The corresponding CBIR analysis results are depicted in Figures 2 (a) and 2 (b). A pure red indicates a high, yellow an average and white a very low similarity. The effects at the upper and left border are due to a dark line in the original image and should be ignored.

The left image shows the similarities of each 10x10 region based on a region lying directly on the seam, emphasizing the intact part of the seam in a strong red. At the edges, it drops gradually towards a bright white. In the central area, the colour is less smooth than in the surrounding parts. Several brighter areas can be spotted and the large crack is represented by a bright line. Above the crack, a small bright spot at the upper edge of the seam can be seen.

The right image takes a segment lying in the centre of the main crack, changing the point-of-view. This does not invert the previous result, but emphasizes the difference of each segment to the fault. In this case, the intact area of the seam is still closer to the crack than the background material. The image is similar to the filtered edge detection image, emphasizing the crack and the vertical seam.

Case two: Multiple cracks and gas pores

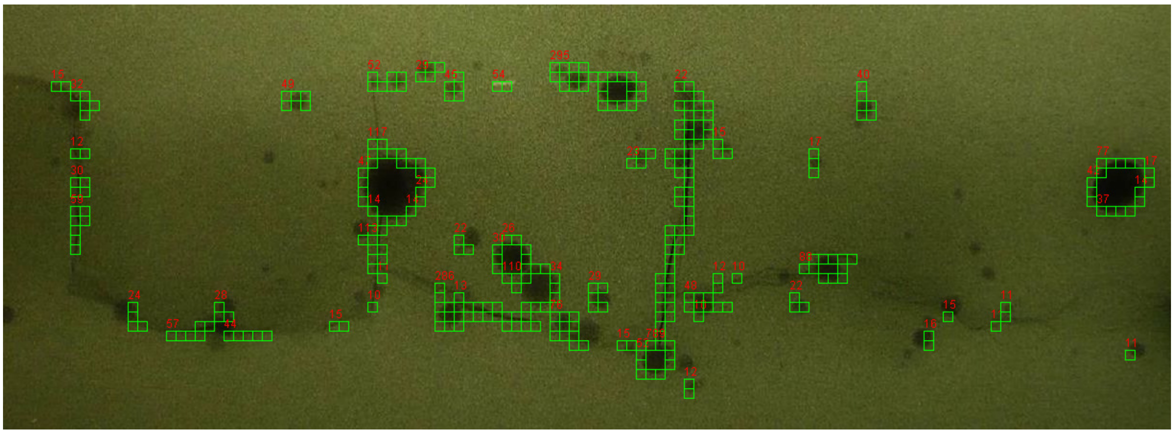

(a) Crack detection results

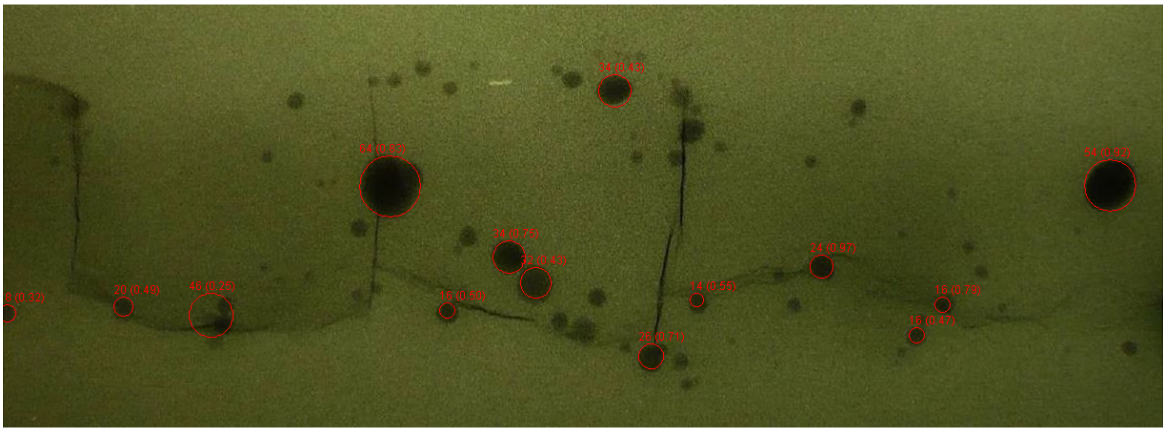

(b) Gas pore detection results

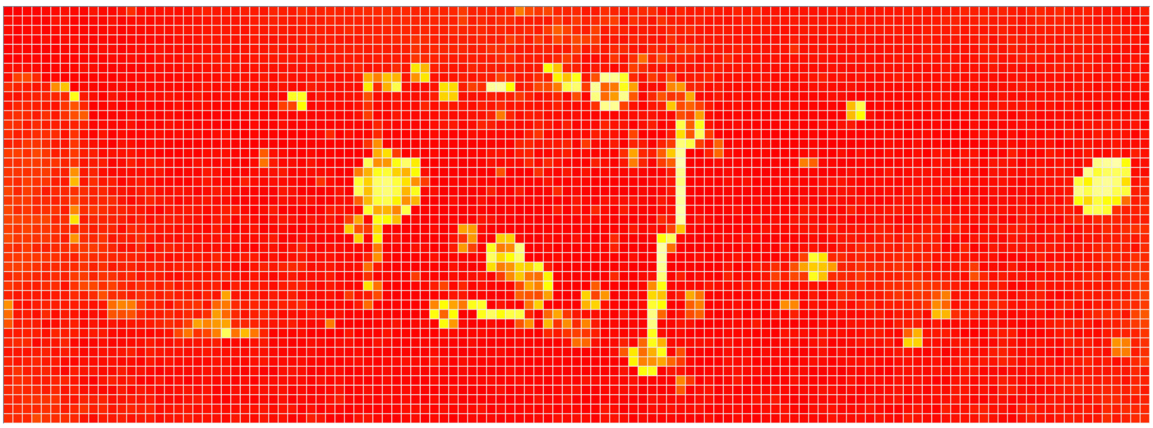

(c) Similarity results based on histogram average

Figure 3: Seam with multiple cracks and gas pores

A second example (fig. 3) contains an x-ray image containing both cracks as well as. The welding seam is interrupted by some transversal cracks, which are connected by a longitudinal one. In addition, the material is interspersed with gaseous inclusions of varying diameter.

The reference crack analysis is depicted in fig. 3 (a). Both the horizontal and the vertical cracks are contained in various clusters. Additionally, the edges of the gas pores are highlighted. In the reference gas pore analysis (fig. 3 (b)), all the major circular defects are detected and measured reasonably well. Several of the less prominent pores as well as the cracks are ignored.

The final image (fig. 3(c)) is the result of the proposed CBIR based analysis. As described above, the image is spilt into several quadratic sections. For each section, a feature vector containing 12 stochastic moments is extracted. The query is then constructed by determining the arithmetic mean of all sections. Sections close to the query are represented in red, a lower similarity by colors gradually changing to yellow and then white. While the majority of the image is red, virtually every defect caused a lower similarity and thus different shade of color. The detected areas-of-interest are the same as detected by the manually fine-tuned detection algorithms.

ANALYSIS AND DISCUSSION

The detailed analysis is carried out on a set of x-ray images of welding seams for two cases: i.e. single crack and Multiple cracks and gas pores.

CASE OF SINGLE CRACK

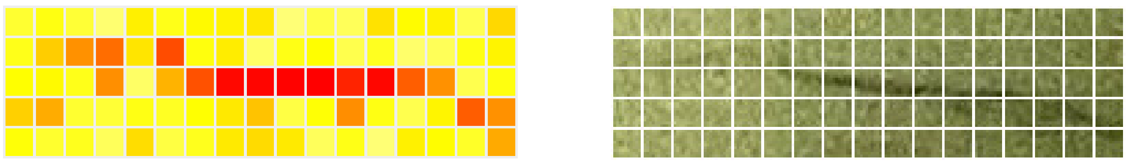

(a) (b)

Figure 4: Detail view of detected crack

Table 1: Similarity values in the surrounding area of the crack

0.40389	0.46589	0.39409	0.27860	0.52891	0.45240	0.50960	0.52321	0.54359	0.26794	0.35854	0.32538	0.55616	0.50440	0.52425	0.34011	0.57458
0.44914	0.59685	0.71392	0.78434	0.54907	0.85068	0.47259	0.53511	0.29895	0.45841	0.50105	0.34819	0.43659	0.29030	0.32701	0.46192	0.52098
0.49840	0.50910	0.45002	0.71777	0.30139	0.64740	0.84042	0.98333	0.98941	0.99524	**1.00000**	0.92962	0.98659	0.81462	0.71557	0.34549	0.46965
0.59154	0.66240	0.40435	0.39358	0.45943	0.43081	0.49668	0.54293	0.61670	0.36619	0.48851	0.72035	0.46164	0.34550	0.51853	0.81761	0.71436
0.48450	0.40852	0.44289	0.32219	0.56588	0.36902	0.44273	0.54061	0.57005	0.54026	0.32127	0.45627	0.26908	0.52606	0.50291	0.42078	0.66518

The results for the largest crack are shown in figure 4. The details of the similarity calculations are presented in table 1 and directly correspond to the 10x10 pixel areas and the respectively displayed color. The query segment achieved the highest similarity of 1.0 (bold font). The arbitrary threshold of 0.6 is chosen to underline the segments that are considered to be related to the crack. A comparison of the crack and its surroundings indicates a strong gradient between the two areas. In most cases, the similarity drops by more than 0.3. This gradient is a further indicator to distinguish between real cracks and generally noisy areas such as seen directly above the crack (fig. 2(a)).

Two other small areas in the image have a high similarity value and a strong difference to their neighbors and are located in the upper boundary line of the seam. These areas may either be defects or image errors, which needs to be checked by an expert. Interestingly, the same three areas also produced from the result image, where the intact seam is highlighted (fig. 2(a)).

The detected crack is comprehensible when comparing the results with the original image. Regarding that the detail level of the original image is not perfect and some noise clutters the background, the achieved accuracy seems to be reasonable. The majority of intact areas achieved similarity values below 0.6 and can be ignored in further processing steps. In the other cases, a closer investigation with a different analysis approach should be applied to classify the segments in detail. In the example presented, the vertical seam is difficult to distinguish from the actual crack, because the results are relatively high.

The results of the other detection approach are quite similar. The main crack has been detected and has been ranked with the highest significance. Other features such as the vertical seam or other suspicious areas have also been found. Yet, further experiments indicated, that the similarity based approach is more robust in varying image conditions. Finding the best parameters for the edge detection algorithm is not trivial and needs to be adjusted for each input image. The approach proposed in this paper only requires an initial query section in order to produce meaningful results, as it spots relative differences, not absolute ones.

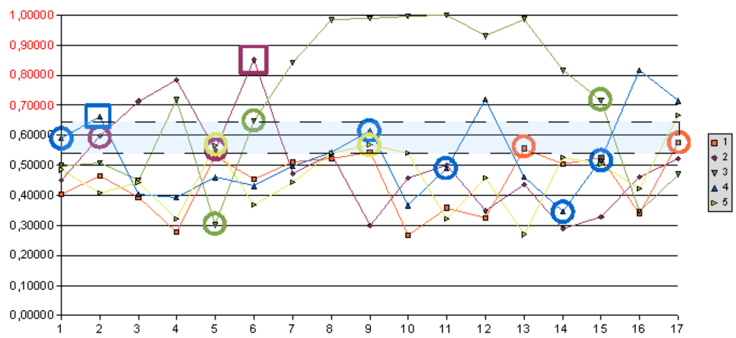

Figure 5: Similarity values in the surrounding area of the crack.

The comparison between the manually assessed sections and the measured similarity results in the surrounding area of the crack is shown in figure 5. Each line stands for a single row. The top row is numbered 1 and the bottom one 5. The x axis describes the width of the area from left (1) to right (17). The similarity values are displayed on the y axis. Two thresholds are set to define the membership between fault (>0.65) and intact (<0.55) area. The space in between represents the area of uncertainty, where no definite conclusion is possible.

The original image is manually assessed and each section is ranked as "faulty", "intact" or "uncertain". The system ranked 69 out of 85 sections identical to the human assessment. In 14 cases, it was unclear either for the human or the system, if a segment is faulty or not (highlighted by circles). In two cases, the automatic result deviates from the human opinion (highlighted by squares).

CASE OF MULTIPLE CRACKS AND GAS PORES

Table 2: Average feature vector

Mean			Variance			Skewness			Correlation		
Red	Green	Blue	Red	Green	Blue	Red	Green	Blue	Red/Green	Red/Blue	Green/Blue
77.2371	82.2430	33.2856	28.8170	29.6430	24.7785	0.0138	0.0051	0.0324	0.9985	0.9451	0.9280

Using the average as query (table 2), a high similarity can be interpreted as a good material quality. Defects can be spotted by searching for low similarities. The background achieved results above 0.8 while the obvious defects (i.e. all defects also spotted by the reference algorithms) are ranked below 0.5.

Both approaches have some difficulty to detect the less prominent parts of the longitudinal crack. In both cases, the threshold between good quality sections and defect sections cannot be set to a distinct value, without losing potentially relevant information. Again, the neighboring regions could be the key for the final decision.

SUMMARY

The single crack case proved its ability to highlight areas of interest without the need of highly specialized algorithms. The results are helpful in drawing the user's attention to faulty areas. Comparing the manual assessment to the threshold based one, only two segments out of 85 are ranked false. In the second case, the use of the average feature vector value for the ranking seems to be a promising approach. Mainly intact samples should lead to a very even distribution of similarities. Yet, the algorithm cannot recognize and ignore unimportant background areas yet.

CONCLUSION AND FUTURE WORK

The proposed methods are easily to be used to cluster radiographic images into different regions-of-interest. It is shown that relevant regions, such as welding seams or cracks can be selected manually to highlight related areas. Also, automatic detection of welding defects is achieved, i.e. an automatic determination of the average query is capable of highlighting regions that deviate from the background, i.e. defects. This may significantly help welding industry in NDT to improve trainees abilities to spot welding defects in training scenarios.

Further research is required to determine the efficiency of other feature vectors. The current work focused on 12 stochastic moments of histograms. Other features may be more efficient in spotting defects, e.g. wavelet-based ones [8].

ACKNOWLEDGEMENTS

This project has been funded with support from the European Commission. This publication reflects the views only of the author, and the Commission cannot be held responsible for any use which may be made of the information contained therein. The authors deeply appreciate the X-Ray samples provided by Miro Uran, Welding Institute, Ljubljana, Slovenia and Luboš Mráz, Welding Research Institute, Bratislava, Slovakia.

REFERENCES

[1] *M Borowski, L Brocker, S Heisterkamp, and J Loffler. Structuring the Visual Content of Digital Libraries Using CBIR Systems. IV '00: Proceedings of the International Conference on Information Visualisation, 00:288, 2000.*

[2] *C Cao, T S Newman, G A Germany, New shape-based auroral oval segmentation driven by LLS-RHT, Pattern Recognition, Volume 42, Issue 5, May 2009, Pages 607-618*

[3] *A Materka and P Cichy, Texture Analysis of X-Ray Image for Detection of Changes in Bone Mass and Structure Institute of Electronics, Technical University of Łódź,*

[4] *R P Pein, M Amador, J Lu and W Renz, Using CBIR and Semantics in 3D-Model Retrieval Computer and Information Technology, 2008. CIT 2008. 8th IEEE International Conference on, 2008, Pages 173-178*

[5] *J Eakins and M Graham, Content-based Image Retrieval, . A Report to the JISC Technology Applications Programme, . University of Northumbria at Newcastle, 1999.*

[6] *R P Pein and Z Lu, Content Based Image Retrieval by Combining Features and Query-By-Sketch. In Arabnia, H. R. & Hashemi, R. R., editors IKE, CSREA Press, 2006, Pages 49-55*

[7] *F A Al-Omari and M A Al-Jarrah, Query by image and video content: a colored-based stochastic model approach Data Knowl. Eng., Elsevier Science Publishers B. V., 2005, 52, 313-332*

[8] *C E Jacobs, A Finkelstein and D H Salesin, Fast Multiresolution Image Querying Computer Graphics, 1995, 29, 277-286*

[9] *S Ribarić, D Marčetić and D S Vedrina, A knowledge-based system for the non-destructive diagnostics of façade isolation using the information fusion of visual and IR images, Expert Systems with Applications, Volume 36, Issue 2, Part 2, March 2009, Pages 3812-3823*

[10] *M K Felisberto, T M Centeno, L Arruda and H Lopes, Automatic Analysis of Radiographic Images for Non Destructive Test Applications Proceedings of 10th SEM International Congress on Experimental and Applied Mechanics, 2004*

[11] *R R da Silva, M Domingo, The state of the art of weld seam radiographic testing Part I, image processing Materials evaluation , 2007, 65, 643-647*

[12] *R R da Silva, M Domingo, The state of the art of weld seam radiographic testing Part II, pattern recognition Materials evaluation , 2007, 65, 833-838*

[13] *I Bartolini, M Patella, WARP: Accurate Retrieval of Shapes Using Phase of Fourier Descriptors and Time Warping Distance IEEE Trans. Pattern Anal. Mach. Intell., IEEE Computer Society, 2005, 27, 142-147*

[14] *Raoul Pascal Pein, Joan Lu and John Birger Stav, An Investigation in Image Retrieval for Analysing Welding Defects, Accepted at Infosci09, Leipzig, April 2009*

[15] *M Schmidt, JIU - The Java Imaging Utilities, [online] http://schmidt.devlib.org/jiu/index.html, 2009*

[16] *R P Pein and Z Lu, A Flexible Image Retrieval Framework. In Y. Shi, G. D. van Albada, J. Dongarra, and P. M. A. Sloot, editors, International Conference on Computational Science (3), volume 4489 of Lecture Notes in Computer Science, Pages 754–761. Springer, 2007.*